Joint planning of distributed generation and electric vehicle charging stations considering real-time charging navigation

4 authors:

Lizi Luo
Nanjing University of Science and Technology
13 PUBLICATIONS   **356** CITATIONS

SEE PROFILE

Wei Gu
Southeast University (China)
293 PUBLICATIONS   **6,770** CITATIONS

SEE PROFILE

Zhi Wu
Southeast University (China)
90 PUBLICATIONS   **2,662** CITATIONS

SEE PROFILE

Suyang Zhou
Southeast University (China)
73 PUBLICATIONS   **1,089** CITATIONS

SEE PROFILE

Some of the authors of this publication are also working on these related projects:

Project   economic dispatch View project

Project   distribution network planning View project

Joint planning of distributed generation and electric vehicle charging stations considering real-time charging navigation

Lizi Luo, Wei Gu*, Zhi Wu, Suyang Zhou

School of Electrical Engineering, Southeast University, Nanjing 210096, China

Abstract—With the popularity of intelligent mobile terminals, as well as the improvement in wireless communication technologies, the application of real-time charging navigation for electric vehicles (EVs) has met a booming development in recent years. Accordingly, more and more EV owners tend to make their charging decisions depending on the guidance from navigation systems, which to some extent transforms the EV charging demands into spatially dispatchable resources in the operation of distribution systems. To involve this spatially dispatchable characteristic at the planning stage of distribution systems, and deploy power devices in a cost-effective way, a comprehensive optimization model concerning the joint planning of distributed generators (DGs) and electric vehicle charging stations (EVCSs) is proposed in this paper from the perspective of a social planner. The proposed joint planning model is embedded with the spatial scheduling problem of EV charging demands, and focuses on the optimum of relevant social costs. To relieve the complexity of the optimization model, an exact second-order cone programming (SOCP) relaxation is utilized to transform the proposed model into the type of mixed integer second-order cone programming (MISOCP), which can be efficiently solved in polynomial time. Finally, a practical urban area coupled with the 33-bus distribution system is used as the test system to implement the proposed approach, and the corresponding allocation schemes as well as annualized social costs are minutely presented. The numerical comparison with traditional Voronoi diagram-based planning methods reveals the significant economic benefits achieved through considering real-time charging navigation technologies.

Keywords—Distributed generation, distribution system, electric vehicle charging navigation, electric vehicle charging station (EVCS), joint planning, mixed integer second-order cone programming (MISOCP).

NOMENCLATURE

Indices

k	EV index
n	Land block index
t	Time segment index
s	Season index
i/j	Bus index

* Corresponding author.
E-mail addresses: luolizi@126.com (L. Luo), wgu@seu.edu.cn (W. Gu), zwu@seu.edu.cn (Z. Wu), suyang.zhou@seu.edu.cn (S. Zhou).

Sets

$u(i)/u(j)$	Downstream buses connected to bus i/j
$v(j)$	Upstream buses connected to bus j
Ω_N	Buses in the distribution system
Ω_L	Branches in the distribution system
$\Omega_{PV/MT/CF}$	Candidate buses of PV/MT/EVCS
$\Omega_{s,i,t}^{EV}$	EVs that head for bus i and intend to be charged at time segment t in season s

Parameters

ir_{rated}	PV rated solar irradiance (W/m^2)
$P_{ir\text{-}rated}$	PV active power output under ir_{rated} (kW)
$S_{PV\text{-}rated}$	PV rated capacity (kVA)
SOC_k	State of charge of electric vehicle k
SOC_{ref}	SOC threshold to find the almost-full EV
Cap_k	Battery capacity of electric vehicle k (kWh)
P_{EV}^{rated}	EV rated charging power (kW)
T_k^{park}	Parking duration of electric vehicle k (h)
N_n	Total number of EVs heading for land block n
N_b	Total number of land blocks in the target area
N_{bus}	Total number of electrical buses in the system
$c_{PV/MT/CF}^I$	Investment cost for per unit PV/MT/CF ($)
d	Discount rate
$y_{PV/MT/CF}$	Economic life of PV/MT/CF (year)
$c_{PV/MT/CF}^{O\&M}$	O&M cost for per unit PV/MT/CF ($)
Δt	Span of each time segment (i.e. 15 minutes in this paper)
c_{MT}^F	Fuel cost for per-unit MT power generation ($/kWh)
c_{em}^C	Tax cost for per-unit CO$_2$ emission ($/g)
ρ_{em}	CO$_2$ emission of per-unit MT power generation (g/kWh)
c^L	Per-unit network losses cost ($/kWh)
R_{ij}/X_{ij}	Resistance/reactance of branch from i to j (Ω)
$N_{s,i}^{ar,WO/WD}$	EVs' arrival number in land block i during the typical workday/weekend in season s
c^T	Per-unit extra traffic cost in charging dispatches ($/km)
d_{ij}	Distance from bus i to bus j (km)
U_{min}/U_{max}	Lower/upper bound of voltage magnitude limit (kV)
$I_{ij,max}$	Permitted maximum current in branch ij (A)

$S_{PV/MT}^{unit}$	Available unit capacity of PV/MT to be installed (kVA)
$Q_{PV,lim}^{unit}$	Maximum limit for the reactive power output of each PV unit (kVar)
d_{lim}	Maximum extra traffic distance accepted by EV owners in charging dispatches (km)

Variables

ir	Solar irradiance (W/m^2)
P_{ir}/Q_{ir}	PV active/reactive power output under ir (kW/kVar)
T_k^{ch}	Required charging time of electric vehicle k (h)
C^I	Annualized investment cost (\$)
$C^{O\&M}$	Annual O&M cost (\$)
C^F	Annual fuel cost (\$)
C^C	Annual CO$_2$ emission cost (\$)
C^L	Annual network losses cost (\$)
C^T	Annual extra traffic cost in charging dispatches (\$)
$R_{PV/MT/CF}$	Auxiliary variable in annualization
$S_{PV,i}^{rated}/S_{MT,i}^{rated}$	Rated capacity of PV/MT installed at bus i (kVA)
$N_i^{PV/MT/CF}$	Integer variable revealing the number of PV/MT/CF installed at bus i
$P_{PV/MT,s,t,i}^{WO/WD}$	PV/MT active power output at bus i under time segment t in the typical workday/weekend of season s (kW)
$I_{s,t,ij}^{WO/WD}$	Current in branch ij at time segment t in the typical workday/weekend of season s (A)
$B_{s,i,k,j}^{WO/WD}$	Binary variable revealing the dispatch scheme for the designated EV in workdays/weekends
$B_{s,i,k,j}$	Unified representation of $B_{s,i,k,j}^{WO}$ and $B_{s,i,k,j}^{WD}$
$P_{s,t,ij}/Q_{s,t,ij}$	Active/reactive power in branch ij at time segment t in season s (kW/kVar)
$U_{s,t,i}$	Voltage magnitude at bus i corresponding to time segment t in season s (kV)
$I_{s,t,ij}$	Unified representation of $I_{s,t,ij}^{WO}$ and $I_{s,t,ij}^{WD}$
$P_{s,t,j}^{eq}/Q_{s,t,j}^{eq}$	Equivalent active/reactive power demands at bus j under time segment t in season s (kW/kVar)
$P_{s,t,j}^{Load}/Q_{s,t,j}^{Load}$	Active/reactive load demand at bus j under time segment t in season s (kW/kVar)
$P_{s,t,j}^{PV}/P_{s,t,j}^{MT}$	Unified representation of $P_{PV,s,t,j}^{WO/WD}/P_{MT,s,t,j}^{WO/WD}$
$P_{s,t,j}^{EV}$	Power demands of EVCS at bus j under time segment t in season s (kW)
$Q_{s,t,j}^{PV}$	PV reactive power output at bus j under time segment t in season s (kVar)
$\bar{U}_{s,t,i}, \bar{I}_{s,t,ij}$	Auxiliary variable employed in the relaxation
$\Delta_{s,t,ij}$	Deviation variable employed to verify the exactness of SOCP relaxation

I. INTRODUCTION

Driven by the anxiety on fossil fuel exhaustion, as well as the economic and environmental concerns of promoting lower-carbon and high efficiency energy utilization, distributed generation and electric vehicles (EVs) have attracted world-wide attention during the past decade [1,2]. Under most circumstances, these emerging elements appear at the end part of power grid, and are integrated into medium/low voltage distribution systems featured with long power-supply distances and weak network structures [3,4]. Consequently, the integration of distributed generation and EVs brings challenges to the reliable operation of distribution systems, and these challenges tend to be more and more intractable as the penetration of distributed generation and EVs booms [5,6]. To be detailed, high penetration of distributed renewable resources always leads to the redundant power back-feeding to upper level networks [7], which is not cost-effective due to the considerable network losses in relatively low voltage levels [8]. While for EVs, the rapid growth of power demand originated from the increasing use of EVs challenges both the economic and security aspects of distribution systems [9]. An efficient way to deal with these challenges is simultaneously deploying distributed generators (DGs) and electric vehicle charging stations (EVCSs) in distribution systems, through which the surplus power generated by DGs can be locally consumed for satisfying EV charging demands [10]. Therefore, it is of great practical significance to explore proper approaches for the joint planning of DGs and EVCSs.

Researches on the planning problems concerning DGs and EVCSs can be found in numerous literatures. These studies are carried out from diverse perspectives and refer to various application scenarios. In [11,12], locations and capacities of selected DGs are optimally allocated in distribution systems with already installed EVCSs. And the uncertainties of EV charging demands are represented by probabilistic method and fuzzy theory, respectively. In [13], the foreseeable growing penetration of EVs are fully considered, and factors like the reinforcement of distribution systems, as well as the reliability criteria are properly involved in determining the configuration schemes of DGs and network topologies. In [14,15], Voronoi diagrams are employed to delimit EVCS service regions, so that each EV in the target area is designated to its nearest EVCS for charging, which apparently extends the modeling methods of EV charging demands in the relevant optimization problems. The emerging concepts of vehicle-to-grid (V2G) and grid-to-vehicle (G2V) are minutely described in [16,17], and the power exchange between grids and EVs is regarded to be bidirectional in the planning model presented in [18], which brings about evident influence on the achieved allocation schemes. In [19], the optimal mix of solar-based DGs and storage units, as well as the charging prices for EVs are determined for maximizing the benefits of EV-parking lots' owners. Furthermore, A comprehensive multi-year distribution system planning framework is proposed in [20], where demand response options are fully considered in the allocation of substations, DGs, feeders, and capacitors. The optimization model that simultaneously deploys DGs and EVCSs is systematically expounded in [21], during which the financial, technical and environmental effects are comprehensively considered. However, EV charging demands are crudely modeled as constants in this optimization process, so that the precision of the planning model is seriously weakened. To

overcome this weakness, time-varying profiles of load demands, DG generation and EV charging demands are fully adopted in [22], and subsequently, the optimization model is formulated as a second-order cone programming (SOCP) problem, which can be effectively solved by appropriate mathematical methods. In [23], a Markov Chain Monte Carlo (MCMC) simulation model is utilized to account for the uncertainties of EV charging demands and DG outputs, based on which the coordinated control strategies of EVs and DGs are embedded into the planning problems. In [24], the simultaneous planning problems of DGs and EVCSs are extended to be multi-objective models, and in consequence, more extensive factors, as well as the economic benefits of different stakeholders are fully considered.

To the best of the authors' knowledge, none of the existing studies have considered the application of real-time charging navigation (i.e. the spatially dispatchable characteristic of EV charging demands) in the planning of DGs and EVCSs. However, with the popularity of intelligent mobile terminals, as well as the improvement in wireless communication technologies, the application of real-time charging navigation has met a booming development in recent years [25,26]. More and more EV owners tend to make their charging decisions depending on the guidance from navigation systems, which to some extent transforms the EV charging demands into spatially dispatchable resources in the operation of distribution systems [27]. This phenomenon challenges the existing planning approaches for power devices in distribution systems, and simultaneously reveals the practical significance of this paper.

To make the description easy to understand, a schematic diagram is provided in Fig. 1 to further explain the aforementioned spatially dispatchable characteristic of EV charging demands. With the application of real-time charging navigation, EVs heading for the destination bus are guided to be charged at nearby EVCSs within a certain geographical distance (i.e. EVCS2, EVCS3 and EVCS6 in Fig. 1). For each EV, selecting which EVCS to implement its charging behavior depends on diverse factors (e.g. the operation state of distribution systems, the sufficiency of charging facilities in EVCSs, the extra traffic cost in charging dispatches and so on), and is essentially an optimization problem embedded into the proposed planning model.
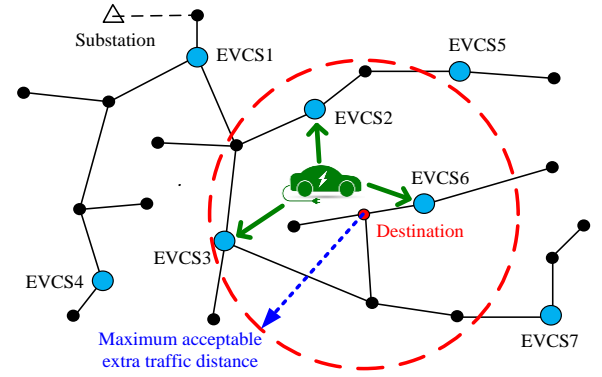

Fig. 1. A schematic diagram of the spatially dispatchable characteristic of EV charging demands

In this paper, a new optimization model is proposed for the joint planning of DGs and EVCSs, through which the optimal sites and sizes of DGs and EVCSs are properly determined. The contributions are summarized as follows.

1) Taking account of the development in real-time charging navigation technologies, EV charging demands are modeled as spatially dispatchable resources in the proposed joint planning model.
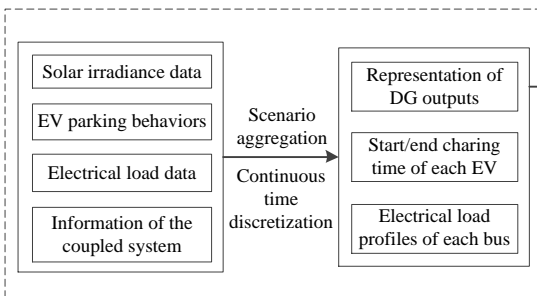
2) The proposed joint planning model is embedded with the spatial scheduling problem of EV charging demands, and the extra traffic cost originated from the dispatches is properly considered as a part of the comprehensive planning objective.

3) An exact SOCP relaxation is employed to transform the proposed model into the type of mixed integer second-order cone programming (MISOCP), which can be ideally solved by off-the-shelf commercial solvers in polynomial time.

4) The proposed research is based on coupled geographical-electrical systems, which is more consistent with practical planning scenarios.

The framework of the proposed research is shown in Fig. 2, and the remaining parts of this paper are organized as follows. Section 2 describes the modeling of DG outputs, EV charging demands and electrical loads. Section 3 formulates the specific optimization model proposed for the joint planning of DGs and EVCSs, as well as the employed SOCP relaxation. Numerical results based on the test system are presented in Section 4. Finally, Section 5 concludes the paper.
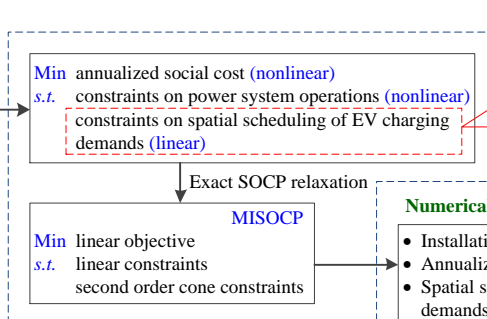
Fig. 2. Framework of the proposed research

II. Modeling of DG Outputs, EV Charging Demands and Electrical Loads

This section presents the modeling methods of DG outputs, EV charging demands and electrical loads in the joint planning problem.

A. Assumptions and simplifications in the modeling

To make the description easy to understand, and meanwhile improve the efficiency of the proposed approach, some assumptions and simplifications have been adopted in the modeling procedure. These assumptions and simplifications are detailedly described in this subsection.

In terms of the selection of DGs, photovoltaic (PV) power plants and micro-turbines (MTs) are selected as the typical representatives of DGs. PV power plants are renewable energy resources that contribute to the reduction of greenhouse gas emission. While the dispatchable characteristic of gas-based MTs plays an important role in the operation of distribution systems.

With respect to EV charging behaviors, only private EVs are considered in this paper, and the destination charging mode [14,28] is assumed to be adopted by EV owners. This assumption is reasonable since it accords with the charging habits of EV owners in urban areas.

Moreover, continuous time periods considered in planning problems always make the established optimization model extremely complicated and hard to be solved. To overcome this difficulty, continuous time periods are divided into discrete ones according to the following simplifications.

1) Eight typical days corresponding to workdays and weekends in four seasons are generated to represent the planning year.

2) Each typical day consists of 96 subdivided time segments (15 minutes each).

3) Each time segment is regarded as a deterministic scenario, that is to say, variations of DG outputs, EV charging demands and electrical loads in each time segment are neglected.

B. Modeling of DG outputs

For PV power plants, solar irradiance is thought to be the most important factor that affects their active power outputs. The distribution curve of solar irradiance in this paper is fitted by historical statistics, which is actually a simple but effective way to represent the temporal variation of solar irradiances. Moreover, due to the obvious seasonality of solar irradiances, the distribution curves corresponding to different seasons are fitted separately. As further explanation, Fig. 3 provides a group of typical distribution curves of solar irradiances, which are derived from public data measured in Seattle, Washington, USA [29]. The solar irradiance is shown in per unit value with the peak solar irradiance employed as the base value.
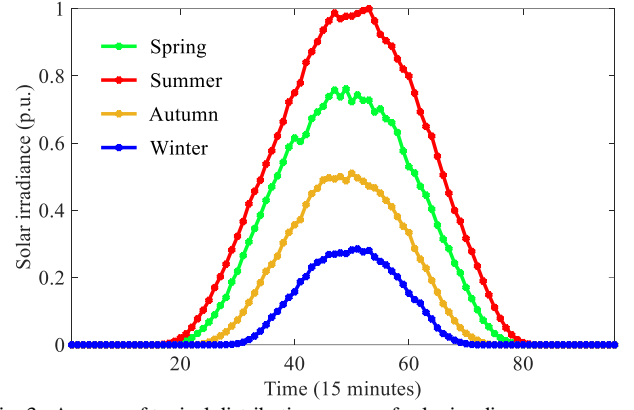

Fig. 3. A group of typical distribution curves of solar irradiances

In the long time-scale planning problems, the relationship between PV active power outputs and solar irradiances can be simplified as a piecewise function [30]:

$$P_{ir} = \begin{cases} P_{ir-rated} \cdot \dfrac{ir}{ir_{rated}}, & 0 \le ir \le ir_{rated} \\ P_{ir-rated}, & ir_{rated} < ir \end{cases} \quad (1)$$

Moreover, with the development in PV-STATCOM technology, more and more PV power plants tend to be utilized as controllable reactive power sources [31]. This new technology makes PV power plants quite useful for voltage control and power factor correction in power systems, both during nighttime and daytime [32,33]. The adjustable ranges of PV reactive outputs can be summarized as (2).

$$-\sqrt{S_{PV-rated}^2 - P_{ir}^2} \le Q_{ir} \le \sqrt{S_{PV-rated}^2 - P_{ir}^2} \quad (2)$$

On the other aspect, gas-based MTs are considered as dispatchable DGs in this paper. Furthermore, MTs are regarded as pure active power sources from the economic perspective, and their actual active power outputs are determined by the optimal scheduling schemes of distribution systems.

C. Modeling of EV charging demands

EV charging demands in certain areas are directly impacted by the corresponding EV parking behaviors, which can be adequately described by distribution curves of EVs' arrival numbers and parking durations [34]. In this paper, to properly fit these distribution curves, historical data of EV parking behaviors are divided into three types according to various land usages of EV destinations (i.e. residential areas, shopping areas and office building areas). And meanwhile, historical data corresponding to workdays and weekends are analyzed separately. The specific curve-fitting processes are consistent with the relevant description in [28], and readers may refer to this literature for more detailed information. Moreover, for the convenience of readers, the typical distribution curves of EVs' arrival numbers and parking durations collected from [28] are attached in Appendix A.

Under destination charging mode, EV owners tend to make their EV batteries as full as possible at each charging time, which is an effective way to relieve their "range anxieties" [35]. Hence, the present state of charge (SOC) is also a

dominant factor that should be considered in the modeling of EV charging demands. SOCs of the arriving EVs are assumed to be uniformly distributed within the interval [0, 1] in this paper. And meanwhile, EVs with extremely high SOCs are treated as almost-full vehicles that do not need charging. To accurately define the aforementioned concept of extremely high, parameter SOC_{ref} is used to represent this SOC threshold, whose numerical value is set to be 0.9 in this paper. Then the required charging time of each EV arriving EVCS can be calculated through (3).

$$T_k^{ch} = \begin{cases} 0, & \text{if } SOC_k \geq SOC_{ref} \\ Cap_k \cdot (1-SOC_k)/P_{EV}^{rated}, & \text{if } Cap_k \cdot (1-SOC_k)/P_{EV}^{rated} \leq T_k^{park} \\ T_k^{park}, & \text{if } Cap_k \cdot (1-SOC_k)/P_{EV}^{rated} > T_k^{park} \end{cases} \tag{3}$$

Finally, a typical distribution of EV charging demands in certain areas can be properly deduced, during which the arrival number and charging time of EVs heading for each land block are specified. The corresponding flowchart is illustrated in Fig. 4.
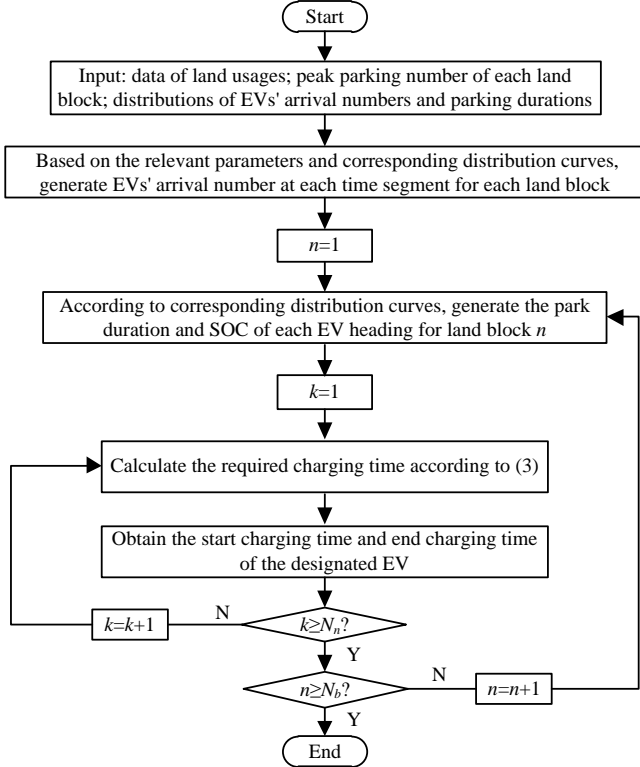

Fig. 4. Flowchart of EV charging demands modeling

D. Modeling of electrical loads

The modeling method of electrical loads presented in [28] is utilized in this paper. Readers may need to refer to [28] for more detailed information. To make it convenient for readers, typical load profiles collected from [28] have been attached in Appendix B.

III. OPTIMIZATION MODEL AND RELAXATION

This section describes the proposed optimization model for the joint planning of DGs and EVCSs, during which the spatially dispatchable characteristic of EV charging demands is properly considered. Subsequently, an exact SOCP relaxation is employed to transform the original mixed integer nonlinear programming (MINLP) problem into the type of MISOCP, and in consequence, the proposed optimization model can be ideally solved by off-the-shelf commercial solvers in polynomial time [36].

A. Objective function

Viewed from the perspective of a social planner, the annualized social cost related with DGs and EVCSs has been properly considered in the objective function. The specific expression of objective function is shown in (4).

$$\min \quad Cost = C^I + C^{O\&M} + C^F + C^C + C^L + C^T \tag{4}$$

where C^I, $C^{O\&M}$, C^F, C^C, C^L and C^T represent the annualized investment cost, annual operation and maintenance (O&M) cost, annual fuel cost, annual CO_2 emission cost, annual network losses cost, and annual extra traffic cost in charging dispatches, respectively. Assuming that each season consists of 65.25 workdays and 26 weekends, then the aforementioned factors can be calculated through (5)-(13).

1) Annualized investment cost:

$$C^I = R_{PV} \cdot \sum_{i=1}^{N_{bus}} (c_{PV}^I \cdot S_{PV,i}^{rated}) + R_{MT} \cdot \sum_{i=1}^{N_{bus}} (c_{MT}^I \cdot S_{MT,i}^{rated}) + R_{CF} \cdot \sum_{i=1}^{N_{bus}} (c_{CF}^I \cdot N_i^{CF}) \tag{5}$$

where the auxiliary variables

$$R_{PV} = \frac{d(1+d)^{y_{PV}}}{(1+d)^{y_{PV}} - 1} \tag{6}$$

$$R_{MT} = \frac{d(1+d)^{y_{MT}}}{(1+d)^{y_{MT}} - 1} \tag{7}$$

$$R_{CF} = \frac{d(1+d)^{y_{CF}}}{(1+d)^{y_{CF}} - 1} \tag{8}$$

2) Annual O&M cost:

$$C^{O\&M} = 65.25 \cdot \sum_{s=1}^{4} \sum_{t=1}^{96} \sum_{i=1}^{N_{bus}} [(c_{PV}^{O\&M} \cdot P_{PV,s,t,i}^{WO} + c_{MT}^{O\&M} \cdot P_{MT,s,t,i}^{WO}) \cdot \Delta t]$$
$$+ 26 \cdot \sum_{s=1}^{4} \sum_{t=1}^{96} \sum_{i=1}^{N_{bus}} [(c_{PV}^{O\&M} \cdot P_{PV,s,t,i}^{WD} + c_{MT}^{O\&M} \cdot P_{MT,s,t,i}^{WD}) \cdot \Delta t] \tag{9}$$
$$+ \sum_{i=1}^{N_{bus}} (c_{CF}^{O\&M} \cdot N_i^{CF})$$

3) Annual fuel cost:

$$C^F = 65.25 \cdot \sum_{s=1}^{4} \sum_{t=1}^{96} \sum_{i=1}^{N_{bus}} [c_{MT}^F \cdot P_{MT,s,t,i}^{WO} \cdot \Delta t]$$
$$+ 26 \cdot \sum_{s=1}^{4} \sum_{t=1}^{96} \sum_{i=1}^{N_{bus}} [c_{MT}^F \cdot P_{MT,s,t,i}^{WD} \cdot \Delta t] \tag{10}$$

4) Annual CO_2 emission cost:

$$C^C = 65.25 \cdot \sum_{s=1}^{4} \sum_{t=1}^{96} \sum_{i=1}^{N_{bus}} [c_{em}^C \cdot P_{MT,s,t,i}^{WO} \cdot \rho_{em} \cdot \Delta t]$$
$$+ 26 \cdot \sum_{s=1}^{4} \sum_{t=1}^{96} \sum_{i=1}^{N_{bus}} [c_{em}^C \cdot P_{MT,s,t,i}^{WD} \cdot \rho_{em} \cdot \Delta t] \tag{11}$$

5) Annual network losses cost:

$$C^L = 65.25 \cdot \sum_{s=1}^{4} \sum_{t=1}^{96} \sum_{i=1}^{N_{bus}} \sum_{j\in u(i)} [c^L \cdot (I_{s,t,ij}^{WO})^2 \cdot R_{ij} \cdot \Delta t]$$
$$+ 26 \cdot \sum_{s=1}^{4} \sum_{t=1}^{96} \sum_{i=1}^{N_{bus}} \sum_{j\in u(i)} [c^L \cdot (I_{s,t,ij}^{WD})^2 \cdot R_{ij} \cdot \Delta t] \quad (12)$$

6) Annual extra traffic cost in charging dispatches:

$$C^T = 65.25 \cdot \sum_{s=1}^{4} \sum_{i=1}^{N_{bus}} \sum_{k=1}^{N_{s,i}^{ar,WO}} \sum_{j\in\Omega_{CF}} [c^T \cdot B_{s,i,k,j}^{WO} \cdot d_{ij}]$$
$$+ 26 \cdot \sum_{s=1}^{4} \sum_{i=1}^{N_{bus}} \sum_{k=1}^{N_{s,i}^{ar,WD}} \sum_{j\in\Omega_{CF}} [c^T \cdot B_{s,i,k,j}^{WD} \cdot d_{ij}] \quad (13)$$

To make the description easy to understand, the authors want to provide more detailed explanation on the variable $B_{s,i,k,j}$, which is a unified representation $B_{s,i,k,j}^{WO}$ and $B_{s,i,k,j}^{WD}$. This variable is a binary one that represents the dispatch scheme for each EV. For the designated EV (i.e. the EV heading for bus i and numbered k in the typical day of season s), $B_{s,i,k,j}$ is valued 1 when the designated EV is guided to be charged in the EVCS at bus j, elsewise $B_{s,i,k,j}$ is valued 0.

B. Constraints

The constraints considered in the proposed optimization model are systematically expounded in this subsection as follows. It should be noted that these constraints are applicable to both workdays and weekends, although they are not described separately for the purpose of concision.

1) Power flow equations:

$$\sum_{i\in v(j)} [P_{s,t,ij} - \frac{(P_{s,t,ij})^2 + (Q_{s,t,ij})^2}{(U_{s,t,i})^2} \cdot R_{ij}] = \sum_{l\in u(j)} P_{s,t,jl} + P_{s,t,j}^{eq} \quad \forall s,t, \quad \forall j\in\Omega_N \quad (14)$$

$$\sum_{i\in v(j)} [Q_{s,t,ij} - \frac{(P_{s,t,ij})^2 + (Q_{s,t,ij})^2}{(U_{s,t,i})^2} \cdot X_{ij}] = \sum_{l\in u(j)} Q_{s,t,jl} + Q_{s,t,j}^{eq} \quad \forall s,t, \quad \forall j\in\Omega_N \quad (15)$$

$$(U_{s,t,j})^2 = (U_{s,t,i})^2 - 2(R_{ij}P_{s,t,ij} + X_{ij}Q_{s,t,ij}) +$$
$$[(R_{ij})^2 + (X_{ij})^2]\frac{(P_{s,t,ij})^2 + (Q_{s,t,ij})^2}{(U_{s,t,i})^2} \quad \forall s,t, \quad \forall ij\in\Omega_L \quad (16)$$

$$(I_{s,t,ij})^2 = \frac{(P_{s,t,ij})^2 + (Q_{s,t,ij})^2}{(U_{s,t,i})^2} \quad \forall s,t, \quad \forall ij\in\Omega_L \quad (17)$$

where the equivalent power demands

$$P_{s,t,j}^{eq} = P_{s,t,j}^{Load} - P_{s,t,j}^{PV} - P_{s,t,j}^{MT} + P_{s,t,j}^{EV} \quad \forall s,t, \quad \forall j\in\Omega_N \quad (18)$$

$$Q_{s,t,j}^{eq} = Q_{s,t,j}^{Load} - Q_{s,t,j}^{PV} \quad \forall s,t, \quad \forall j\in\Omega_N \quad (19)$$

2) Voltage magnitude restrictions:

$$U_{min} \le U_{s,t,i} \le U_{max} \quad \forall s,t, \quad \forall i\in\Omega_N \quad (20)$$

3) Branch current restrictions:

$$|I_{s,t,ij}| \le I_{ij,max} \quad \forall s,t, \quad \forall ij\in\Omega_L \quad (21)$$

4) Discrete size constraints for DGs:

$$S_{PV,i}^{rated} = N_i^{PV} \cdot S_{PV}^{unit} \quad \forall i\in\Omega_{PV} \quad (22)$$

$$S_{MT,i}^{rated} = N_i^{MT} \cdot S_{MT}^{unit} \quad \forall i\in\Omega_{MT} \quad (23)$$

5) Regulations on MTs' outputs:

$$0 \le P_{s,t,i}^{MT} \le S_{MT,i}^{rated} \quad \forall s,t, \quad \forall i\in\Omega_{MT} \quad (24)$$

6) Regulations on PV reactive outputs:

$$-N_i^{PV} \cdot Q_{PV,lim}^{unit} \le Q_{s,t,i}^{PV} \le N_i^{PV} \cdot Q_{PV,lim}^{unit} \quad \forall s,t, \quad \forall i\in\Omega_{PV} \quad (25)$$

In each time segment, $Q_{PV,lim}^{unit}$ is a constant relevant with solar irradiance, and can be calculated according to (2).

7) Regulations on the dispatches of EVs:

$$\sum_{j\in\Omega_{CF}} B_{s,i,k,j} = 1 \quad \forall s,k \quad \forall i\in\Omega_N \quad (26)$$

$$B_{s,i,k,j} = 0 \quad \forall s,k, \quad \forall(i,j)\in\{(i,j)\,|\,d_{ij} > d_{lim}\} \quad (27)$$

During the dispatch of EVs, each EV must be assigned to one and only one EVCS, as defined in (26). Furthermore, viewed from the aspect of convenience, dispatch schemes which bring about extra traffic distances exceeding d_{lim} are regarded to be unacceptable by EV owners, and thereby the corresponding binary variables are set to be 0 in (27).

8) Power demands due to EV charging behaviors:

$$P_{s,t,j}^{EV} = P_{EV}^{rated} \cdot (\sum_{i=1}^{N_{bus}} \sum_{k\in\Omega_{s,i,t}^{EV}} B_{s,i,k,j}) \quad \forall s,t, \quad \forall j\in\Omega_{CF} \quad (28)$$

To make the description easy to understand, the authors want to provide more detailed explanation on the set $\Omega_{s,i,t}^{EV}$. In the typical day of season s, during all the EVs heading for bus i, only those whose charging periods (i.e. from start charging time to end charging time) cover the target time segment t are included in $\Omega_{s,i,t}^{EV}$.

9) Sufficiency of EV charging facilities (CFs):

$$N_j^{CF} \ge \sum_{i=1}^{N_{bus}} \sum_{k\in\Omega_{s,i,t}^{EV}} B_{s,i,k,j} \quad \forall s,t, \quad \forall j\in\Omega_{CF} \quad (29)$$

At each bus, the quantity of charging facilities installed in EVCS should be greater than that of EV charging demands at any time segment.

C. SOCP relaxation

The standard form of SOCP is shown in (30), which is minutely described in [37].

$$\min \quad f^T x$$
$$s.t. \quad \|A_i x + b_i\|_2 \le c_i^T x + d_i, \quad i = 1, 2, \cdots, m \quad (30)$$
$$F x = g$$

where $x\in\mathbb{R}^n$ stands for the optimization variable vector, and $f\in\mathbb{R}^n$, $A_i\in\mathbb{R}^{n_i\times n}$, $b_i\in\mathbb{R}^{n_i}$, $c_i\in\mathbb{R}^n$, $d_i\in\mathbb{R}$, $F\in\mathbb{R}^{p\times n}$, $g\in\mathbb{R}^p$ are problem parameters.

To accord with the aforementioned standard form of SOCP, some variable substitutions are implemented to the proposed planning model in this paper, as described in (31) and (32).

$$\bar{U}_{s,t,i} = (U_{s,t,i})^2 \quad (31)$$

$$\bar{I}_{s,t,ij} = (I_{s,t,ij})^2 \quad (32)$$

After variable substitutions, constraints (14)-(17) and (20)-(21) are reformulated as (33)-(38).

$$\sum_{i\in v(j)} [P_{s,t,ij} - \bar{I}_{s,t,ij} \cdot R_{ij}] = \sum_{l\in u(j)} P_{s,t,jl} + P_{s,t,j}^{eq} \quad \forall s,t, \quad \forall j\in\Omega_N \quad (33)$$

$$\sum_{i\in v(j)} [Q_{s,t,ij} - \bar{I}_{s,t,ij} \cdot X_{ij}] = \sum_{l\in u(j)} Q_{s,t,jl} + Q_{s,t,j}^{eq} \quad \forall s,t, \quad \forall j\in\Omega_N \quad (34)$$

$$\bar{U}_{s,t,j} = \bar{U}_{s,t,i} - 2(R_{ij}P_{s,t,ij} + X_{ij}Q_{s,t,ij})$$
$$+ [(R_{ij})^2 + (X_{ij})^2] \cdot \bar{I}_{s,t,ij} \quad \forall s,t, \quad \forall ij\in\Omega_L \quad (35)$$

$$\bar{I}_{s,t,ij} = \frac{(P_{s,t,ij})^2 + (Q_{s,t,ij})^2}{\bar{U}_{s,t,i}} \quad \forall s,t, \quad \forall ij\in\Omega_L \quad (36)$$

$$(U_{min})^2 \le \bar{U}_{s,t,i} \le (U_{max})^2 \quad \forall s,t, \quad \forall i\in\Omega_N \quad (37)$$

$$\bar{I}_{s,t,ij} \le (I_{ij,max})^2 \quad \forall s,t, \quad \forall ij\in\Omega_L \quad (38)$$

Subsequently, through replacing the equals sign with greater than or equal to sign, (36) is relaxed to be (39), which is equivalent to the second order cone expression shown in (40).

$$\bar{I}_{s,t,ij} \geq \frac{(P_{s,t,ij})^2 + (Q_{s,t,ij})^2}{\bar{U}_{s,t,i}} \quad \forall s,t, \quad \forall ij \in \Omega_L \quad (39)$$

$$\left\| \begin{array}{c} 2P_{s,t,ij} \\ 2Q_{s,t,ij} \\ \bar{I}_{s,t,ij} - \bar{U}_{s,t,i} \end{array} \right\|_2 \leq \bar{I}_{s,t,ij} + \bar{U}_{s,t,i} \quad \forall s,t, \quad \forall ij \in \Omega_L \quad (40)$$

Finally, the proposed planning model after relaxation is shown in (41), which belongs to the type of MISOCP and can be efficiently solved by off-the-shelf commercial solvers in polynomial time [36].

$$\begin{aligned} \min \quad & (4) \\ s.t. \quad & (18)(19)(22)-(29)(33)-(35)(37)(38)(40) \end{aligned} \quad (41)$$

The relaxation from (36) to (39) is proved to be an exact one on the premise of some conditions [37]. The proposed planning model in this paper is properly satisfied with these particular conditions, and thereby the employed SOCP relaxation does not impact the accuracy of the joint planning problem.

IV. CASE STUDY

In this section, a practical urban area coupled with the 33-bus distribution system [38] is used as the test system to implement the proposed model and approach. The optimization models after relaxation are effectively solved through commercial solver CPLEX, which is called by YALMIP toolbox under MATLAB environment. Based on the numerical results, allocation schemes of DGs and EVCSs are comprehensively analyzed, and meanwhile the comparison study with traditional Voronoi diagram-based planning methods is provided.

A. Test system and parameter settings

The test system employed in this paper is a coupled one consisting of both geographical and electrical information, as shown in Fig. 5. The geographical information is derived from a practical urban area in Jiangsu, China, while the electrical information of the 33-bus distribution system can be found in [38]. For convenience, the load type of each electrical bus is regarded to be consistent with the corresponding land usage, as marked by different colors. Moreover, electrical buses and EVs' destinations are supposed to be located at geometrical centers of the land blocks. Thereby, the extra traffic distance in charging dispatches can be obtained through the distance measurements between relevant geometrical centers.

Parameters used in this paper are specified as follows.

1) The distribution curves of solar irradiances are derived from public data [29] and thoroughly shown in Fig. 3. The peak solar irradiance is set to be 1000 W/m² in this paper.

2) The distribution curves of EVs' arrival numbers and parking durations are collected from [28] and completely displayed in Appendix A. While the peak parking number of each land block is shown in Appendix C, which is estimated on the basis of the corresponding annual peak load.
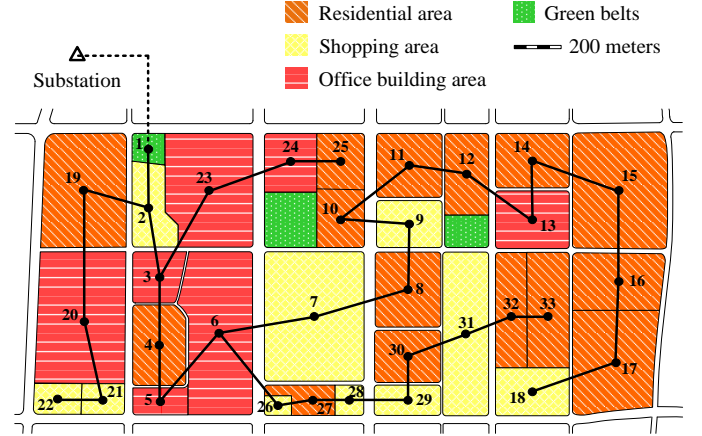

Fig. 5. A practical urban area coupled with the 33-bus distribution system

3) Electrical load profiles used in this paper are classified according to diverse scenarios, as shown in Appendix B. These data are collected from [28].

4) The available unit capacities of PV and MT are set to be 10 kVA, while the rated charging power of CF in EVCS is valued as 30 kW [28].

5) Parameters related to DGs and CFs are collected from [28] and [37]. Their specific values are shown in Table I.

TABLE I
PARAMETERS OF DGs AND CFs

	PV [37]	MT [37]	CF [28]
Economic life	25 years	10 years	10 years
Investment cost	1200 $/kVA	750 $/kVA	3250 $/suit
O&M cost	2 $/MWh	10 $/MWh	325 $/suit/year
Fuel cost	N/A	120 $/MWh	N/A
CO_2 emission	N/A	720 g/kWh	N/A
CO_2 emission tax	N/A	10 $/t	N/A

6) Candidate bus sets for the deployments of PV, MT and EVCS are defined as {6, 12, 15, 17, 21, 24, 30, 32}, {4, 7, 16, 18, 22, 25, 29, 31} and {2, 7, 10, 14, 17, 21, 31}, respectively.

7) The EV battery capacity is assumed to be 100 kWh [28].

8) The discount rate is specified to be 0.03 [28].

9) Per-unit network losses cost is valued 80 $/MWh [28], while the per-unit extra traffic cost in charging dispatches is set as 0.5 $/km.

10) Lower and upper bounds of voltage magnitude limits are respectively set as 0.9 p.u. and 1.1 p.u.. Moreover, the test system is a three-phase balanced distribution system, and the permitted maximum branch current of each phase is assumed to be 400 A.

11) In charging dispatches, the maximum extra traffic distance accepted by EV owners is set to be 0.6 km.

B. Numerical results

Based on the aforementioned test system and parameters, optimal allocation schemes of DGs and EVCSs, as well as the relevant costs are acquired by the proposed approach, as concretely shown in Table II. In addition, for the purpose of future comparison, this study is denoted as Base Case.

TABLE II
OPTIMAL SOLUTIONS OF THE JOINT PLANNING PROBLEM UNDER BASE CASE

Candidate buses	PV capacities (kVA)	MT capacities (kVA)	Quantity of CFs in EVCS
2	0	0	11
7	0	0	37
10	0	0	21
12	10	0	0
14	0	0	10
15	440	0	0
17	300	0	10
18	0	140	0
21	0	0	12
31	0	0	19
32	430	0	0
Total installation	1180	140	120
C^I ($\times 10^5$ \$)	1.3935		
$C^{O\&M}$ ($\times 10^4$ \$)	4.3047		
C^F ($\times 10^2$ \$)	6.4550		
C^C ($\times 10^1$ \$)	3.8730		
C^L ($\times 10^4$ \$)	5.9478		
C^T ($\times 10^4$ \$)	2.0820		
Annualized social cost ($\times 10^5$ \$)	2.6338		

As observed in Table II, totally 1180 kVA PV arrays, 140 kVA gas-based MTs, and 120 EV charging facilities are installed in the test system, with annualized social cost of 2.6338×10^5 \$. Viewed from the perspective of DGs, the allocated capacity of PV power plants is obviously larger than that of MTs, which thanks to the excellent economic performance of PV generation. And meanwhile, most DGs tend to be installed at the end-parts of feeders with long power-supply distances. Deploying DGs in such way can bring about more significant effects in the improvement of voltage profiles, as well as the reduction in related operation costs of distribution systems. Moreover, with regard to the allocation of EVCSs, proper quantities of CFs are installed at all the EVCS candidate buses, which makes the target areas fully covered with EV charging service and thereby the charging demands of EV owners can be satisfied in a convenient way.

C. Comparison study

Among the existing works regarding EVCS planning problems, the spatially dispatchable characteristic of EV charging demands is always neglected, and EVs heading for a certain geographical range are unalterably designated to the corresponding EVCS according to the Voronoi diagram-based service region delimitation [14,15]. In this subsection, a Comparative Case derived from the existing studies is generated for the purpose of highlighting the benefits of the proposed model and approach. To be specific, CFs are deployed at all the EVCS candidate buses under the Comparative Case and their service regions determined by Voronoi diagrams are shown in Fig. 6. Optimal solutions of the joint planning problem under Comparative Case are thoroughly shown in Table III. The comparison between Base Case and Comparative Case are provided in Fig. 7 and Fig. 8, from the aspects of allocation schemes and economic benefits, respectively.
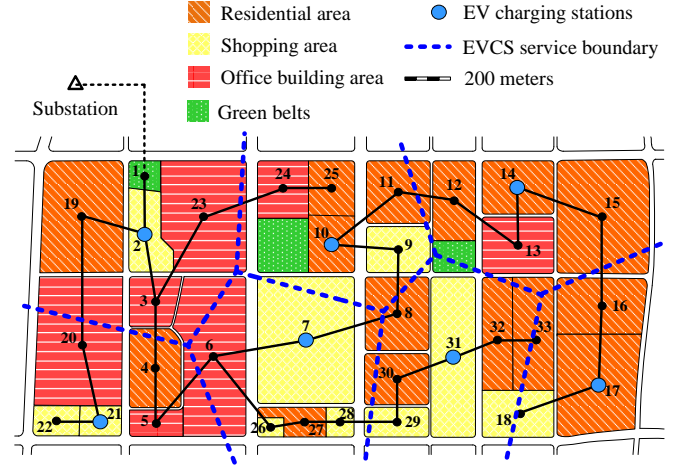

Fig. 6. Voronoi diagram-based EVCS service regions in Comparative Case

Totally 1460 kVA PV arrays, 240 kVA gas-based MTs, and 130 EV charging facilities are installed in Comparative Case, which are significantly more than those of Base Case. In consequence, the annualized social cost under Comparative Case is inevitably larger than that of Base Case. To be detailed, the annualized social cost under Comparative Case is 3.0252×10^5 \$, which is nearly 15% greater than that of Base Case. These increments can be observed in most of the cost items except for C^T, due to the intrinsic property of Voronoi diagrams. In fact, on the basis of the Voronoi diagram-based service region delimitation of EVCS, all the EVs in Comparative Case are designated to their nearest CFs.
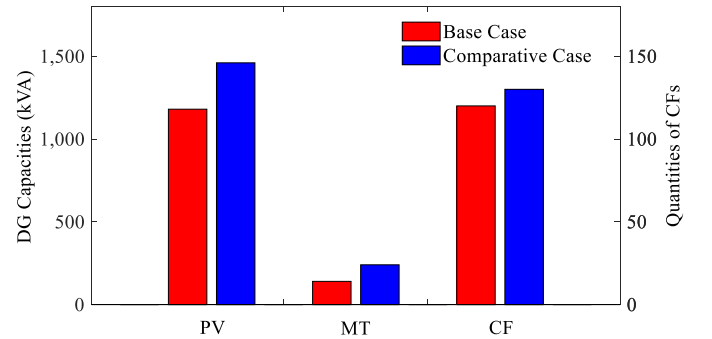

Fig. 7. Comparison on total allocation capacities/quantities of DGs and CFs
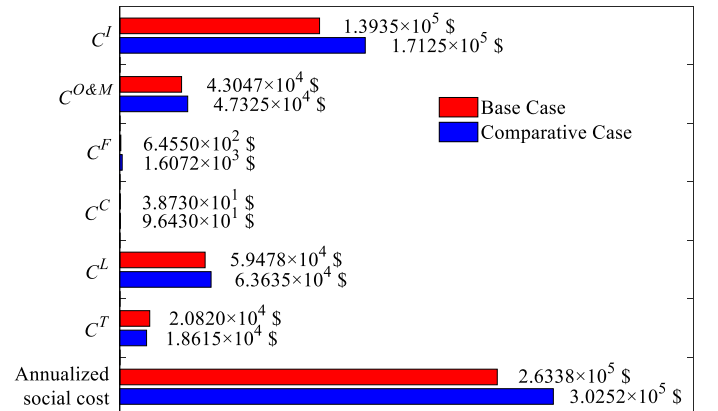

Fig. 8. Comparison on various cost items

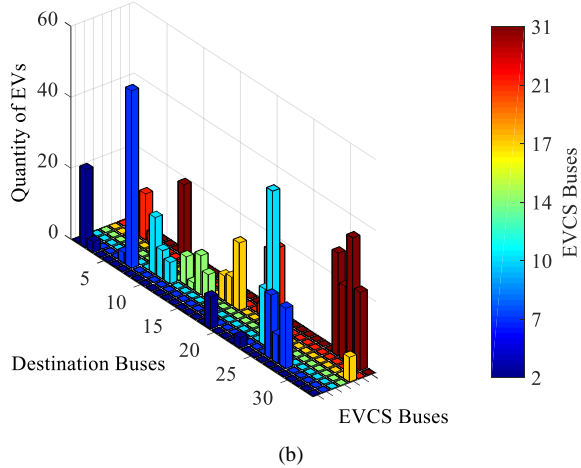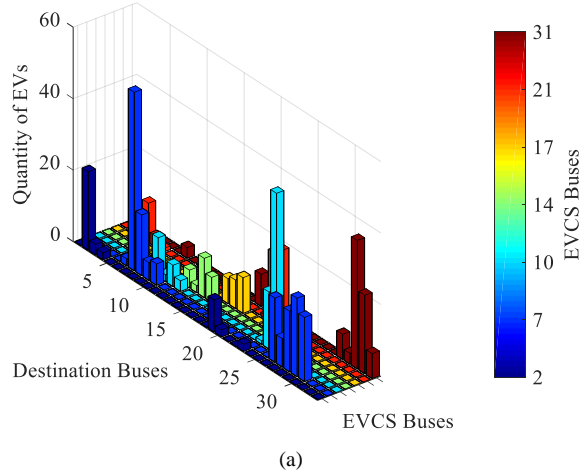| Candidate buses	PV capacities (kVA)	MT capacities (kVA)	Quantity of CFs in EVCS
2	0	0	11
7	0	0	20
10	0	0	24
14	0	0	16
15	540	0	0
17	470	0	18
18	0	240	0
21	0	0	15
31	0	0	26
32	450	0	0
Total installation	1460	240	130
C^I ($\times 10^5$ \$)	1.7125		
$C^{O\&M}$ ($\times 10^4$ \$)	4.7325		
C^F ($\times 10^3$ \$)	1.6072		
C^C ($\times 10^1$ \$)	9.6430		
C^L ($\times 10^4$ \$)	6.3635		
C^T ($\times 10^4$ \$)	1.8615		
Annualized social cost ($\times 10^5$ \$)	3.0252		

(a)

(b)

Fig. 9. Traffic flows of EV charging behaviors at the typical weekend in Summer. (a) under Base Case; (b) under Comparative Case

According to the aforementioned numerical results, as well as the corresponding comparisons, benefits of taking into consideration the real-time charging navigation technologies during the joint planning of DGs and EVCSs are effectively verified. These benefits can be explained from two aspects. On the one hand, the spatially dispatchable characteristic of EV charging demands enhances the relevance among different EVCSs. This strengthened relevance helps to reduce the total installation number of CFs in the target area, since the peak charging demands of EVs heading for land blocks with various land usages always occur at different time. On the other hand, with the spatial scheduling of EV charging demands embedded into the joint planning problems, EVs tend to be charged at more appropriate electrical buses, which contributes to the reductions on DG installations, network losses, as well as some other operation-related costs. To describe this phenomenon in a more direct way, the specific traffic flows of EV charging behaviors under Base Case and Comparative Case are provided in Fig. 9, where the typical day corresponding to weekends in Summer is selected as an example. As observed in Fig. 9, with consideration of the spatially dispatchable characteristic of EV charging demands, distinctly more EVs are charged in EVCSs connected to the front-parts of electrical feeders (e.g. bus 2 and bus 7), and meanwhile the quantity of EVs charged at the end-parts of electrical feeders (e.g. bus 17 and bus 31) decreases significantly.

In summary, the utilization of real-time charging navigation technologies effectively relieves EV charging demands' negative impacts on distribution systems. Taking this factor into consideration during the planning stage would apparently reduce the total installation capacity/quantity of DGs and EV charging facilities, as well as some operation-related costs. As results, the proposed model and approach can bring significant reduction in the annualized social costs of allocation schemes, and thereby act as potentially valuable tools for social planners in practical planning scenario.

D. Exactness of SOCP relaxation

Deviation variables are introduced in this subsection to test the exactness of SOCP relaxation employed in this paper, whose expressions are shown in (42).

$$\Delta_{s,t,ij} = \left| \overline{I}_{s,t,ij} - \frac{(P_{s,t,ij})^2 + (Q_{s,t,ij})^2}{\overline{U}_{s,t,i}} \right| \quad \forall s,t, \quad \forall ij \in \Omega_L \qquad (42)$$
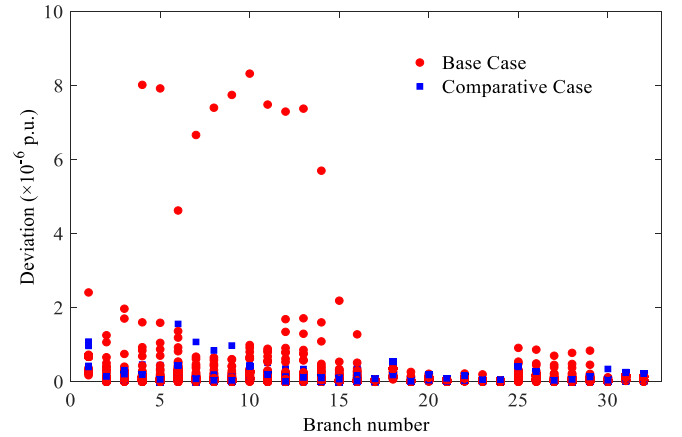

Fig. 10. Distributions of deviation variables

The numerical values of deviation variables are calculated according to (42), and their distributions are shown in Fig. 10.

As observed in Fig. 10, deviations of SOCP relaxation in this paper are in the order of 10^{-6}, which are quite small and can be regarded as reasonable errors in numerical calculations. Thereby, relaxation from (36) to (39) is proved to be an exact procedure, and does not impact the accuracy of the proposed model and approach.

E. Sensitivity analysis

The economic benefits achieved in the proposed model and approach are largely impacted by parameter settings. In this subsection, different values of d_{lim} and c^T are tested in Base Case and Comparative Case. The comparisons are specifically shown in Fig. 11.
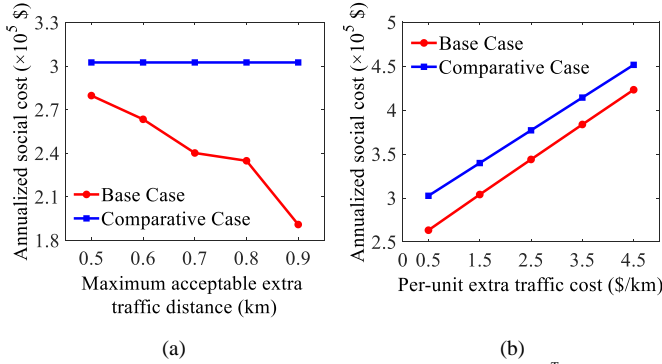

Fig. 11. Sensitivity analysis on parameter settings. (a) d_{lim}; (b) c^T

For d_{lim}, the maximum acceptable extra traffic distance is valued from 0.5 km to 0.9 km in this subsection. It can be observed that the annualized social costs under Base Case decrease distinctly along with the growth of d_{lim}. While for Comparative Case, these costs keep at a constant. This phenomenon is reasonable as the growth of d_{lim} extends the options of EV charging demand dispatches in Base Case. As results, the relevance among different EVCSs is further strengthened and EV charging demands can be satisfied at more appropriate electrical buses. While for Comparative Case, EVs heading for a certain geographical range are designated to a particular EVCS, and thereby the optimal allocation schemes of DGs and EVCSs are independent from d_{lim}.

For c^T, the per-unit extra traffic cost is changed from 0.5 \$/km to 4.5 \$/km in this subsection. Along with the growth of c^T, annualized social costs corresponding to both Base Case and Comparative Case are with obvious increments. Regarding Comparative Case, the increment is linear since the fluctuation of c^T does not impact the traffic flow of EV charging behaviors. While for Base Case, the annualized social costs are acquired through optimization processes, and their rising is faster than that of Comparative Case. In other words, with regard to the joint planning of DGs and EVCSs, the economic benefits of considering the spatially dispatchable characteristic of EV charging demands become more and more inconspicuous along with the growth of c^T. This phenomenon is easy to understand as extremely high traffic costs substantially enforce EV owners to charge their EVs at nearest EVCSs.

V. CONCLUSION

This paper proposes an optimization model for jointly determining the allocation schemes of distributed generators (DGs) and electric vehicle charging stations (EVCSs), during which the spatially dispatchable characteristic of electric vehicle charging demands is fully considered. The proposed model is transformed into the type of mixed integer second-order cone programming through an exact relaxation, and thereby can be efficiently solved in polynomial time. To demonstrate the effectiveness of the proposed model and approach, a coupled geographical-electrical system is used as the test system, and the main conclusions are summarized as follows.

1) The proposed model and approach can effectively solve the joint planning problems of DGs and EVCSs considering real-time charging navigation. The optimal sites and sizes of DGs and EVCSs can be properly determined at the planning stage.

2) Regarding electric vehicle charging demands as spatially dispatchable resources would reduce the total installation capacity/quantity of DGs and electric vehicle charging facilities, as well as some operation-related costs. As results, allocating DGs and EVCSs based on the proposed model and approach can bring about significant economic benefits.

3) The economic benefits originated from the consideration of real-time charging navigation are largely impacted by some parameters (e.g. maximum acceptable extra traffic distance d_{lim} and per-unit extra traffic cost c^T). When electric vehicle owners accept to be dispatched within a longer distance with lower per-unit extra traffic cost, more significant benefits would be achieved.

However, electric vehicle owners in the proposed study are assumed to be entirely rational and unconditionally obey the guidance from navigation systems. This assumption largely simplifies the joint planning problems but simultaneously makes the proposed model not completely consistent with practical scenarios. In the future work, the uncertainties in the decision-making of electric vehicle owners (e.g. the probability and degree of their violating navigation systems) will be properly considered, and the joint planning model of DGs and EVCSs will be further extended to achieve better practical value.

APPENDIX

A. Typical distributions of EVs' arrival numbers and parking durations

Fig. 12 and Fig. 13 reveal the typical distribution curves of EVs' arrival numbers and parking durations collected from [28].

B. Typical load profiles

Fig.14 illustrates the typical load profiles collected from [28].

C. EVs' peak parking number of each land block

For each land block, EVs' peak parking number is provided in Table IV.

TABLE IV
EVs' PEAK PARKING NUMBER OF EACH LAND BLOCK

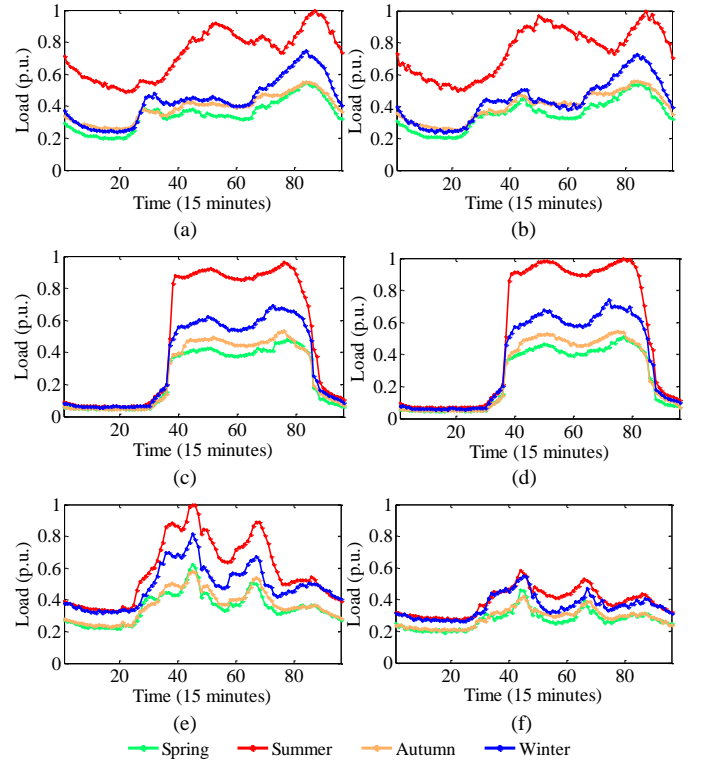| Block number	EVs' peak parking number	Block number	EVs' peak parking number
1	0	18	5
2	6	19	5
3	5	20	5
4	7	21	5
5	4	22	5
6	4	23	5
7	12	24	25
8	12	25	25
9	4	26	4
10	4	27	4
11	3	28	4
12	4	29	7
13	4	30	12
14	7	31	9
15	4	32	13
16	4	33	4
17	4		

Fig. 14. Typical load profiles of different scenarios. (a) workdays in residential areas; (b) weekends in residential areas; (c) workdays in shopping areas; (d) weekends in shopping areas; (e) workdays in office building areas; (f) weekends in office building areas [28]
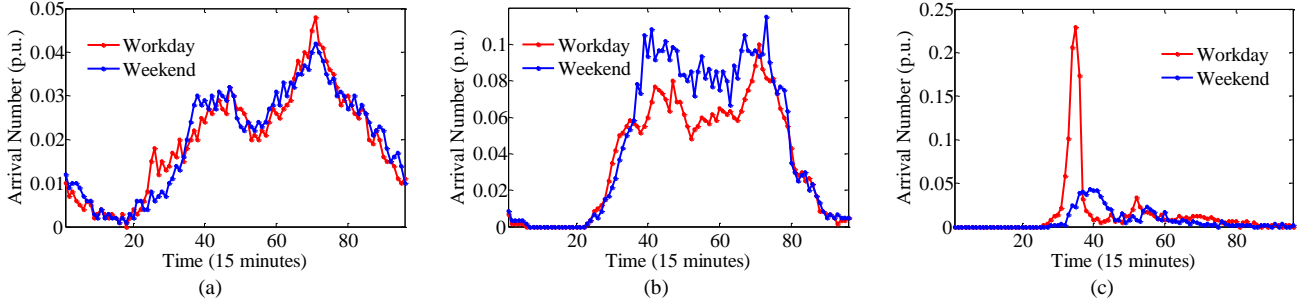

Fig. 12. Typical distribution of EVs' arrival numbers. (a) residential area; (b) shopping area; (c) office building area [28]
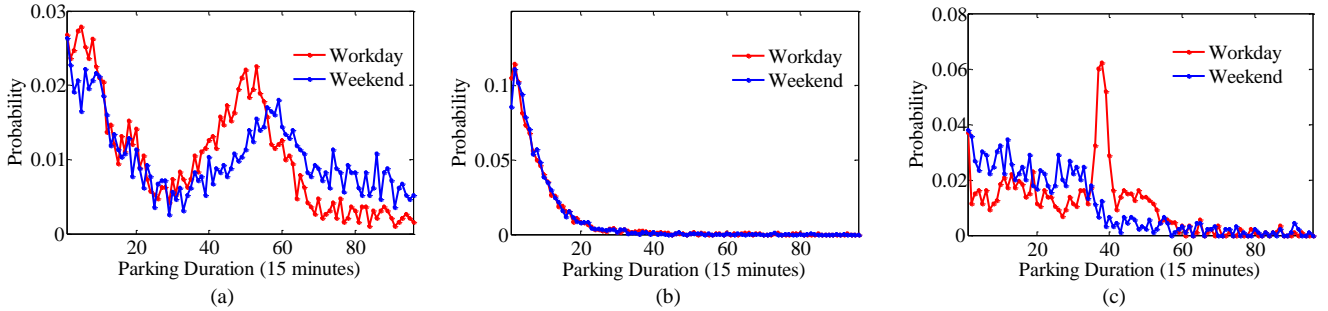

Fig. 13. Typical distribution of EVs' parking durations. (a) residential area; (b) shopping area; (c) office building area [28]

REFERENCES

[1] Bahrami S, Amini MH. A decentralized trading algorithm for an electricity market with generation uncertainty. Appl Energy 2018;218:520-32.

[2] Zheng M, Wang X, Meinrenken CJ, Ding Y. Economic and environmental benefits of coordinating dispatch among distributed electricity storage. Appl Energy 2018;210:842-55.

[3] Zhang S, Cheng H, Li K, Tai N, Wang D, Li F. Multi-objective distributed generation planning in distribution network considering correlations among uncertainties. Appl Energy 2018;226:743-55.

[4] Kazemi MA, Sedighizadeh M, Mirzaei MJ, Homaee O. Optimal siting and sizing of distribution system operator owned EV parking lots. Appl Energy 2016;179:1176-84.

[5] Veldhuis AJ, Leach M, Yang A. The impact of increased decentralised generation on the reliability of an existing electricity network. Appl Energy 2018;215:479-502.

[6] Yagcitekin B, Uzunoglu M. A double-layer smart charging strategy of electric vehicles taking routing and charge scheduling into account. Appl Energy 2016;167:407-19.

[7] Li H, Eseye AT, Zhang J, Zheng D. Optimal energy management for industrial microgrids with high-penetration renewables. Prot Control Mod Power Syst 2017;2:12.

[8] Walling RA, Saint R, Dugan RC, Burke J, Kojovic LA. Summary of distributed resources impact on power delivery systems. IEEE Trans Power Deliv 2008;23(3):1636-44.

[9] Mu Y, Wu J, Jenkins N, Jia H, Wang C. A spatial–temporal model for grid impact analysis of plug-in electric vehicles. Appl Energy 2014;114:456-65.

[10] Fazelpour F, Vafaeipour M, Rahbari O, Rosen MA. Intelligent optimization to integrate a plug-in hybrid electric vehicle smart parking lot with renewable energy resources and enhance grid characteristics. Energy Convers Manage 2014;77:250-61.

[11] Ahmadian A, Sedghi M, Elkamel A, Aliakbar-Golkar M, Fowler M. Optimal WDG planning in active distribution networks based on possibilistic–probabilistic PEVs load modelling. IET Gener Transm Distrib 2017;11(4):865-75.

[12] Ahmadian A, Sedghi M, Aliakbar-Golkar M. Fuzzy load modeling of plug-in electric vehicles for optimal storage and DG planning in active distribution network. IEEE Trans Veh Technol 2017;66(5):3622-31.

[13] Zeng B, Feng J, Zhang J, Liu Z. An optimal integrated planning method for supporting growing penetration of electric vehicles in distribution systems. Energy 2017;126:273-84.

[14] Zhang H, Hu Z, Xu Z, Song Y. An integrated planning framework for different types of PEV charging facilities in urban area. IEEE Trans Smart Grid 2016;7(5):2273-84.

[15] Liu Z, Wen F, Ledwich G. Optimal planning of electric-vehicle charging stations in distribution systems. IEEE Trans Power Deliv 2013;28(1):102-10.

[16] Mozafar MR, Amini MH, Moradi MH. Innovative appraisement of smart grid operation considering large-scale integration of electric vehicles enabling V2G and G2V systems. Electr Power Syst Res 2018;154:245-56.

[17] Cai H, Chen Q, Guan Z, Huang J. Day-ahead optimal charging/discharging scheduling for electric vehicles in microgrids. Prot Control Mod Power Syst 2018;3:9.

[18] Atia R, Yamada N. More accurate sizing of renewable energy sources under high levels of electric vehicle integration. Renew Energy 2015;81:918-25.

[19] Awad ASA, Awad MFS, El-Fouly THM, El-Saadany EF, Salama MMA. Optimal resource allocation and charging prices for benefit maximization in smart PEV-parking lots. IEEE Trans Sustain Energy 2017;8(3):906-15.

[20] Humayd ASB, Bhattacharya K. Distribution system planning to accommodate distributed energy resources and PEVs. Electr Power Syst Res 2017;145:1-11.

[21] Pazouki S, Mohsenzadeh A, Ardalan S, Haghifam M. Simultaneous planning of PEV charging stations and DGs considering financial, technical, and environmental effects. Can J Electr Comput Eng 2015;38(3):238-45.

[22] Erdinç O, Taşçıkaraoğlu A, Paterakis NG, Dursun İ, Sinim MC, Catalão JPS. Comprehensive optimization model for sizing and siting of DG units, EV charging stations and energy storage systems. IEEE Trans Smart Grid 2018;9(4):3871-82.

[23] Kandil SM, Farag HEZ, Shaaban MF, El-Sharafy MZ. A combined resource allocation framework for PEVs charging stations, renewable energy resources and distributed energy storage systems. Energy 2018;143:961-72.

[24] Amini MH, Moghaddam MP, Karabasoglu O. Simultaneous allocation of electric vehicles' parking lots and distributed renewable resources in smart power distribution networks. Sustain Cities Soc 2017;28:332-42.

[25] Guo Q, Xin S, Sun H, Li Z, Zhang B. Rapid-charging navigation of electric vehicles based on real-time power systems and traffic data. IEEE Trans Smart Grid 2014;5(4):1969-79.

[26] Tan J, Wang L. Real-time charging navigation of electric vehicles to fast charging stations: A hierarchical game approach. IEEE Trans Smart Grid 2017;8(2):846-56.

[27] Amini MH, Karabasoglu O. Optimal operation of interdependent power systems and electrified transportation networks. Energies 2018;11(1):196.

[28] Luo L, Gu W, Zhou S, Huang H, Gao S, Han J, Wu Z, Dou X. Optimal planning of electric vehicle charging stations comprising multi-types of charging facilities. Appl Energy 2018;226:1087-99.

[29] UO Solar Radiation Monitoring Laboratory. Available: http://solardat.uoregon.edu/download/MthAvg/SEMAQ14.txt.

[30] Liu Z, Wen F, Ledwich G. Optimal siting and sizing of distributed generators in distribution systems considering uncertainties. IEEE Trans Power Deliv 2011;26(4):2541-51.

[31] AlKaabi SS, Khadkikar V, Zeineldin HH. Incorporating PV inverter control schemes for planning active distribution networks. IEEE Trans Sustain Energy 2015;6(4):1224-33.

[32] Varma RK, Khadkikar V, Seethapathy R. Nighttime application of PV solar farm as STATCOM to regulate grid voltage. IEEE Trans Energy Convers 2009;24(4):983-5.

[33] Varma RK, Rahman SA, Vanderheide T. New control of PV solar farm as STATCOM (PV-STATCOM) for increasing grid power transmission limits during night and day. IEEE Trans Power Deliv 2015;30(2):755-63.

[34] Zhang H, Hu Z, Xu Z, Song Y. Optimal planning of PEV charging station with single output multiple cables charging spots. IEEE Trans Smart Grid 2017;8(5):2119-28.

[35] Dong J, Liu C, Lin Z. Charging infrastructure planning for promoting battery electric vehicles: An activity-based approach using multiday travel data. Transp Res Part C 2014;38:44-55.

[36] Xing H, Cheng H, Zhang Y, Zeng P. Active distribution network expansion planning integrating dispersed energy storage systems. IET Gener Transm Distrib 2016;10(3):638-44.

[37] Luo L, Gu W, Zhang X, Cao G, Wang W, Zhu G, You D. Optimal siting and sizing of distributed generation in distribution systems with PV solar farm utilized as STATCOM (PV-STATCOM). Appl Energy 2018;210:1092-100.

[38] Baran ME, Wu FF. Network reconfiguration in distribution systems for loss reduction and load balancing. IEEE Trans Power Deliv 1989;4(2):1401-7.